EUROPEAN ORGANISATION FOR NUCLEAR RESEARCH

CERN-PPE/92-139
17 August 1992

A Search for Doubly-Charged Higgs Production in Z^0 Decays

The OPAL Collaboration

Abstract

A search for the decay of the Z^0 into doubly-charged Higgs bosons ($H^{\pm\pm}$) decaying to same-sign lepton pairs is presented using data collected with the OPAL detector at LEP, with an integrated luminosity of 6.8 pb^{-1}. Four-track final states from prompt decays, and events with at least one highly ionizing track from long-lived $H^{\pm\pm}$ were sought. $H^{\pm\pm}$ are excluded in the mass range from zero to 45.6 GeV/c^2 and for a coupling constant range that extends down to zero.

(Submitted to Physics Letters B)

The OPAL Collaboration

P.D. Acton[25], G. Alexander[23], J. Allison[16], P.P. Allport[5], K.J. Anderson[9], S. Arcelli[2], A. Astbury[28], D. Axen[29], G. Azuelos[18,a], G.A. Bahan[16], J.T.M. Baines[16], A.H. Ball[17], J. Banks[16], R.J. Barlow[16], S. Barnett[16], J.R. Batley[5], G. Beaudoin[18], A. Beck[23], J. Becker[10], T. Behnke[27], K.W. Bell[20], G. Bella[23], P. Berlich[10], S. Bethke[11], O. Biebel[3], U. Binder[10], I.J. Bloodworth[1], P. Bock[11], B. Boden[3], H.M. Bosch[11], S. Bougerolle[29], H. Breuker[8], R.M. Brown[20], A. Buijs[8], H.J. Burckhart[8], C. Burgard[27], P. Capiluppi[2], R.K. Carnegie[6], A.A. Carter[13], J.R. Carter[5], C.Y. Chang[17], D.G. Charlton[8], P.E.L. Clarke[25], I. Cohen[23], J.C. Clayton1, W.J. Collins[5], J.E. Conboy[15], M. Cooper[22], M. Coupland[14], M. Cuffiani[2], S. Dado[22], G.M. Dallavalle[2], S. De Jong[8], L.A. del Pozo[5], H. Deng[17], A. Dieckmann[11], M. Dittmar[4], M.S. Dixit[7], E. do Couto e Silva[12], J.E. Duboscq[8], E. Duchovni[26], G. Duckeck[11], I.P. Duerdoth[16], D.J.P. Dumas[6], P.A. Elcombe[5], P.G. Estabrooks[6], E. Etzion[23], H.G. Evans[9], F. Fabbri[2], M. Fincke-Keeler[28], H.M. Fischer[3], D.G. Fong[17], M. Foucher[17], A. Gaidot[21], O. Ganel[26], J.W. Gary[4], J. Gascon[18], R.F. McGowan[16], N.I. Geddes[20], C. Geich-Gimbel[3], S.W. Gensler[9], F.X. Gentit[21], G. Giacomelli[2], V. Gibson[5], W.R. Gibson[13], J.D. Gillies[20], J. Goldberg[22], M.J. Goodrick[5], W. Gorn[4], C. Grandi[2], F.C. Grant[5], J. Hagemann[27], G.G. Hanson[12], M. Hansroul[8], C.K. Hargrove[7], P.F. Harrison[13], J. Hart[8], P.M. Hattersley[1], M. Hauschild[8], C.M. Hawkes[8], E. Heflin[4], R.J. Hemingway[6], R.D. Heuer[8], J.C. Hill[5], S.J. Hillier[1], T. Hilse[10], D.A. Hinshaw[18], J.D. Hobbs[8], P.R. Hobson[25], D. Hochman[26], R.J. Homer[1], A.K. Honma[28,a], C.P. Howarth[15], R.E. Hughes-Jones[16], R. Humbert[10], P. Igo-Kemenes[11], H. Ihssen[11], D.C. Imrie[25], A.C. Janissen[6], A. Jawahery[17], P.W. Jeffreys[20], H. Jeremie[18], M. Jimack[2], M. Jobes[1], R.W.L. Jones[13], P. Jovanovic[1], C. Jui[4], D. Karlen[6], K. Kawagoe[24], T. Kawamoto[24], R.K. Keeler[28], R.G. Kellogg[17], B.W. Kennedy[15], S. Kluth[5], T. Kobayashi[24], T.P. Kokott[3], S. Komamiya[24], L. Köpke[8], J.F. Kral[8], R. Kowalewski[6], J. von Krogh[11], J. Kroll[9], M. Kuwano[24], P. Kyberd[13], G.D. Lafferty[16], F. Lamarche[18], J.G. Layter[4], P. Le Du[21], P. Leblanc[18], A.M. Lee[17], M.H. Lehto[15], D. Lellouch[26], P. Lennert[11], C. Leroy[18], J. Letts[4], S. Levegrün[3], L. Levinson[26], S.L. Lloyd[13], F.K. Loebinger[16], J.M. Lorah[17], B. Lorazo[18], M.J. Losty[7], X.C. Lou[12], J. Ludwig[10], M. Mannelli[8], S. Marcellini[2], G. Maringer[3], C. Markus[3], A.J. Martin[13], J.P. Martin[18], T. Mashimo[24], P. Mättig[3], U. Maur[3], J. McKenna[28], T.J. McMahon[1], J.R. McNutt[25], F. Meijers[8], D. Menszner[11], F.S. Merritt[9], H. Mes[7], A. Michelini[8], R.P. Middleton[20], G. Mikenberg[26], J. Mildenberger[6], D.J. Miller[15], R. Mir[12], W. Mohr[10], C. Moisan[18], A. Montanari[2], T. Mori[24], M. Morii[24], T. Mouthuy[12,b], B. Nellen[3], H.H. Nguyen[9], M. Nozaki[24], S.W. O'Neale[8,c], F.G. Oakham[7], F. Odorici[2], H.O. Ogren[12], C.J. Oram[28,a], M.J. Oreglia[9], S. Orito[24], J.P. Pansart[21], B. Panzer-Steindel[8], P. Paschievici[26], G.N. Patrick[20], N. Paz-Jaoshvili[23], P. Pfister[10], J.E. Pilcher[9], J.L. Pinfold[g], D. Pitman[28], D.E. Plane[8], P. Poffenberger[28], B. Poli[2], A. Pouladdej[6], E. Prebys[8], T.W. Pritchard[13], H. Przysiezniak[18], G. Quast[27], M.W. Redmond[9], D.L. Rees[1], G.E. Richards[16], D. Robinson[8], A. Rollnik[3], J.M. Roney[9], E. Ros[8], S. Rossberg[10], A.M. Rossi[2,d], M. Rosvick[28], P. Routenburg[6], K. Runge[10], O. Runolfsson[8], D.R. Rust[12], M. Sasaki[24], C. Sbarra[8], A.D. Schaile[10], O. Schaile[10], W. Schappert[6], P. Scharff-Hansen[8], P. Schenk[28], H. von der Schmitt[11], S. Schreiber[3], C. Schwick[27], J. Schwiening[3], W.G. Scott[20], M. Settles[12], T.G. Shears[5], B.C. Shen[4], C.H. Shepherd-Themistocleous[7], P. Sherwood[15], R. Shypit[29], A. Simon[3], P. Singh[13], G.P. Siroli[2], A. Skuja[17], A.M. Smith[8], T.J. Smith[8], G.A. Snow[17], R. Sobie[28,e], R.W. Springer[17], M. Sproston[20], K. Stephens[16], J. Steuerer[28], R. Ströhmer[11], D. Strom[30], T. Takeshita[24,f], P. Taras[18], S. Tarem[26], M. Tecchio[9], P. Teixeira-Dias[11], N. Tesch[3], N.J. Thackray[1], G. Transtromer[25], N.J. Tresilian[16], T. Tsukamoto[24], M.F. Turner[5], G. Tysarczyk-Niemeyer[11], D. Van den plas[18], R. Van Kooten[8], G.J. VanDalen[4], G. Vasseur[21], C.J. Virtue[7], A. Wagner[27], D.L. Wagner[9], C. Wahl[10], J.P. Walker[1], C.P. Ward[5], D.R. Ward[5], P.M. Watkins[1], A.T. Watson[1], N.K. Watson[8], M. Weber[11], P. Weber[6], S. Weisz[8], P.S. Wells[8], N. Wermes[11], M.A. Whalley[1], G.W. Wilson[4], J.A. Wilson[1], V-H. Winterer[10], T. Wlodek[26], S. Wotton[11], T.R. Wyatt[16], R. Yaari[26], A. Yeaman[13], G. Yekutieli[26], M. Yurko[18], W. Zeuner[8], G.T. Zorn[17].

[1]School of Physics and Space Research, University of Birmingham, Birmingham, B15 2TT, UK
[2]Dipartimento di Fisica dell' Università di Bologna and INFN, Bologna, 40126, Italy
[3]Physikalisches Institut, Universität Bonn, D-5300 Bonn 1, FRG
[4]Department of Physics, University of California, Riverside, CA 92521 USA
[5]Cavendish Laboratory, Cambridge, CB3 0HE, UK
[6]Carleton University, Dept of Physics, Colonel By Drive, Ottawa, Ontario K1S 5B6, Canada
[7]Centre for Research in Particle Physics, Carleton University, Ottawa, Ontario K1S 5B6, Canada
[8]CERN, European Organisation for Particle Physics, 1211 Geneva 23, Switzerland
[9]Enrico Fermi Institute and Department of Physics, University of Chicago, Chicago Illinois 60637, USA
[10]Fakultät für Physik, Albert Ludwigs Universität, D-7800 Freiburg, FRG
[11]Physikalisches Institut, Universität Heidelberg, Heidelberg, FRG
[12]Indiana University, Dept of Physics, Swain Hall West 117, Bloomington, Indiana 47405, USA
[13]Queen Mary and Westfield College, University of London, London, E1 4NS, UK
[14]Birkbeck College, London, WC1E 7HV, UK
[15]University College London, London, WC1E 6BT, UK
[16]Department of Physics, Schuster Laboratory, The University, Manchester, M13 9PL, UK
[17]Department of Physics and Astronomy, University of Maryland, College Park, Maryland 20742, USA
[18]Laboratoire de Physique Nucléaire, Université de Montréal, Montréal, Quebec, H3C 3J7, Canada
[20]Rutherford Appleton Laboratory, Chilton, Didcot, Oxfordshire, OX11 0QX, UK
[21]DPhPE, CEN Saclay, F-91191 Gif-sur-Yvette, France
[22]Department of Physics, Technion-Israel Institute of Technology, Haifa 32000, Israel
[23]Department of Physics and Astronomy, Tel Aviv University, Tel Aviv 69978, Israel
[24]International Centre for Elementary Particle Physics and Dept of Physics, University of Tokyo, Tokyo 113, and Kobe University, Kobe 657, Japan
[25]Brunel University, Uxbridge, Middlesex, UB8 3PH UK
[26]Nuclear Physics Department, Weizmann Institute of Science, Rehovot, 76100, Israel
[27]Universität Hamburg/DESY, II Inst für Experimental Physik, 2000 Hamburg 52, Germany
[28]University of Victoria, Dept of Physics, P O Box 3055, Victoria BC V8W 3P6, Canada
[29]University of British Columbia, Dept of Physics, 6224 Agriculture Road, Vancouver BC V6T 1Z1, Canada
[30]University of Oregon, Dept of Physics, Eugene, Oregon 97403, USA

[a]Also at TRIUMF, Vancouver, Canada V6T 2A3
[b]Now at Centre de Physique des Particules de Marseille, Faculté des Sciences de Luminy, Marseille
[c]On leave from Birmingham University, Birmingham B15 2TT, UK
[d]Now at Dipartimento di Fisica, Università della Calabria and INFN, 87036 Rende, Italy
[e]And IPP, McGill University, High Energy Physics Department, 3600 University Str, Montreal, Quebec H3A 2T8, Canada
[f]Also at Shinshu University, Matsumoto 390, Japan
[g]Now at Dept of Physics, University of Alberta, Edmonton, T6G 2J1, Canada

1 Introduction

The existence of a doubly-charged Higgs boson ($H^{\pm\pm}$) is a novel feature of some models that extend the Standard Model to allow small neutrino mass [1, 2, 3], or that explore different possibilities for the Higgs sector [4].

Since the $H^{\pm\pm}$ does not couple to quarks, there are three modes by which the $H^{\pm\pm}$ can decay: by Yukawa couplings to like-sign lepton pairs ($H^{\pm\pm} \rightarrow \ell_1^{\pm}\ell_2^{\pm}$, where $\ell_{1,2} = e, \mu, \tau$), by the weak decay mode ($H^{\pm\pm} \rightarrow H^{\pm}W^{\pm}$), or by the Higgs decay mode ($H^{\pm\pm} \rightarrow H^{\pm}H^{\pm}$ and $H^{\pm}H^{\pm}H^{0}$). For pair-produced $H^{\pm\pm}$ that could be observed at LEP, the large value of the mass of singly-charged Higgs bosons imposed by existing limits [5] leads to a suppression of both the weak and Higgs decay modes due to limited phase space and the presence of one or more virtual bosons in the decay products. The importance of the Higgs decay mode is likely to be further reduced because of the expected small values of the coupling constants involved [4, 6]. In this publication it will be assumed that the $H^{\pm\pm}$ decays solely via Yukawa couplings to like-sign lepton pairs.

The leptonic decay mode of the $H^{\pm\pm}$ gives rise to final states containing four charged leptons. The large coupling of the $H^{\pm\pm}$ to the Z^0 and the distinctive four-lepton final state make LEP a promising place to search for the doubly-charged Higgs boson. If the $H^{\pm\pm}$ decays dominantly to same-sign lepton pairs with a coupling constant less than 10^{-7}, the $H^{\pm\pm}$ will have a lifetime that is long enough for it to decay well away from the interaction point.

Neglecting radiative corrections, the expression for the Z^0 partial width for decays into $H^{\pm\pm}$ pairs (following [6]) is:

$$\Gamma(Z^0 \rightarrow H^{++}H^{--}) = \frac{G_F M_Z^3}{6\pi\sqrt{2}}(I_3^L - Q\sin^2\theta_W)^2(1 - \frac{4M_H^2}{M_Z^2})^{\frac{3}{2}}, \quad (1)$$

where M_Z is the mass of the Z^0 boson, $\sin^2\theta_W$ is the electroweak mixing parameter, G_F is the Fermi coupling constant and M_H, Q, I_3^L are the mass, charge and third component of weak isospin respectively of the $H^{\pm\pm}$. The value of I_3^L is model dependent, and can take any of the three possible values 1, 0 or -1. This width would correspond to a sizeable fraction of the total Z^0 width, comparable to $\Gamma(Z^0 \rightarrow \mu^+\mu^-)$ for low mass $H^{\pm\pm}$.

The $H^{\pm\pm}$ partial width to decay to two charged leptons ℓ, ℓ' depends on the coupling constant $g_{\ell\ell'}$. The analysis described in this paper gives different exclusion regions for different values of the coupling constant matrix with elements $g_{\ell\ell'}$ for two reasons. The first is that the $H^{\pm\pm}$ lifetime depends on $g_{\ell\ell'}$, and the search is sensitive to the lifetime. Secondly, since the event topology sought has low multiplicity, the search is less sensitive to $H^{\pm\pm}$ decays that include taus due to the value of BR($\tau \rightarrow$ one charged track). Results are presented for the case $H^{\pm\pm} \rightarrow \tau\tau$, which has the smallest exclusion region. Other cases, for which other elements of the coupling constant matrix are non-zero yield larger exclusion regions. The region for one such case, $H^{\pm\pm} \rightarrow$ ee or $\mu\mu$, is also presented.

The partial width for $H^{\pm\pm}$ to decay to leptons of the same family is given by [7] :

$$\Gamma(H^{\pm\pm} \rightarrow \ell^{\pm}\ell^{\pm}) = \sum_{\ell=e,\mu,\tau} \frac{g_{\ell\ell}{}^2 M_H}{8\pi}\left[1 - \frac{2m_\ell^2}{M_H^2}\right]\left[1 - \frac{4m_\ell^2}{M_H^2}\right]^{\frac{1}{2}}. \quad (2)$$

where $g_{\ell\ell}$ are the unknown Yukawa coupling constants, and m_ℓ is the mass of the leptons.

Previous limits on the doubly-charged Higgs boson [7], [8] have been given usually in terms of the coupling strengths of the Higgs boson to lepton pairs ($g_{\ell\ell}$) and of the $H^{\pm\pm}$ mass. The most stringent

limits (at the 90% confidence level) result from a search in e^+e^- collisions [9] that excludes a Higgs boson with $I_3^L = 1$ with a mass in the range $6.6 < M_H < 36.5$ GeV/c^2 and $g_{\ell\ell} > 3 \times 10^{-7}$. The corresponding limit for Higgs bosons with $I_3^L = 0$ excludes the mass range $7.3 < M_H < 34.3$ GeV/c^2 for the same $g_{\ell\ell}$ interval.

For values of $g_{\ell\ell}$ smaller than approximately 10^{-7}, the efficiency to detect $H^{\pm\pm} \rightarrow \ell_1^\pm \ell_2^\pm$ decreases due to the long decay length of the $H^{\pm\pm}$. At very small $g_{\ell\ell}$ ($\sim 10^{-8} - 10^{-9}$), the doubly-charged Higgs boson could often traverse the OPAL tracking chambers without decaying. $Z^0 \rightarrow H^{++}H^{--}$ events could then have a back-to-back topology in the tracking chamber, or else a final state with one track – corresponding to a doubly-charged Higgs boson – recoiling against a $H^{\pm\pm}$ that may decay to two leptons somewhere within the tracking chambers. The highly ionizing doubly-charged $H^{\pm\pm}$ track would have a distinctively large energy loss per unit length (dE/dx). In using equation (2) to calculate decay lengths for long-lived $H^{\pm\pm}$ the coupling constant matrix was taken to have elements $g_{ee} = g_{\mu\mu} = g_{\tau\tau}$ and $g_{\ell\ell'} = 0, \ell \neq \ell'$. This choice is arbitrary, and is used to define $g_{\ell\ell}$ for the long lifetime analysis.

The data used in this analysis were recorded at LEP during 1990 using the OPAL detector. The integrated luminosity for this period was 6.8 pb^{-1}. The data were collected in an energy scan at and around the Z^0 mass. This sample includes roughly 145 000 events identified as hadronic decays of the Z^0. Numbers of produced $H^{\pm\pm}$ were predicted, as a function of mass and $|I_3^L|$, by incorporating equation (1) into the formalism for the calculation of pair-production of scalar particles [10], which includes corrections for initial state radiation. The number of $H^{\pm\pm}$ pair events expected for this energy scan is given in Table 1 as a function of mass. Searches were made for the above event topologies in the data. Efficiencies for these searches for signal events were calculated, and limits determined using the numbers of observed and calculated events. The difference between the Standard Model prediction and measurements of Γ_{Z^0} was also used to establish mass limits for the $H^{\pm\pm}$.

2 The OPAL detector

The OPAL detector [11] is a multipurpose apparatus having an acceptance of nearly 4π steradians. The central detector consists of a system of tracking chambers inside a 0.435 T solenoidal magnetic field. The central detector system is surrounded by a time-of-flight counter array (TOF), a lead glass electromagnetic calorimeter (EM) with a presampler, an instrumented magnet return yoke serving as a hadron calorimeter, four layers of outer muon chambers, and low-angle forward detectors. The parts of the detector relevant to this search are now briefly described.

The central tracking detector consists of a precision vertex chamber, a large volume "jet" chamber, and chambers for tracking in the r-θ plane (the coordinate system is defined with z-axis increasing along the electron beam axis, θ and ϕ being the polar and azimuthal angles). The main tracking is done with the jet chamber, a drift chamber of approximately four meters length and two meters radius, with 24 sectors in ϕ and 159 axial layers of sense wires in each sector. Tracks with $|\cos\theta| < 0.97$ have a minimum of 20 possible hits in the jet chamber. For each hit, three-dimensional coordinates are determined from the wire position, the drift time and from a charge division measurement. The integrated charge is measured for each hit at both ends of each wire. Their sum is used to calculate the energy loss (dE/dx) of the particle in the chamber gas. For a well measured track traversing the full radial extent of the jet chamber giving 159 charge samples, the resolution, $\sigma_{dE/dx}/(dE/dx)$, is 3.8% for a typical minimum ionizing track in a hadronic event.

The electromagnetic calorimeter consists of a cylindrical array of 9440 lead glass blocks 24.6 radi-

ation lengths deep covering the range $|\cos\theta| < 0.82$ (the barrel region), and 2264 lead glass blocks 20 radiation lengths deep in the endcaps covering the region $0.82 < |\cos\theta| < 0.98$ (the endcap region). Each block subtends a solid angle of approximately 40×40 mrad^2 and projects towards a point near the interaction point in the barrel region, and points along the beam direction in the endcap region. The electromagnetic calorimeter covers 98% of the solid angle.

The TOF apparatus consists of 160 scintillator bars each 4.5 cm thick and 6.84 m long, at a mean radius of 2.36 m, covering $|\cos\theta| < 0.82$ and 2π in azimuth. The flight time resolution is 0.5 ns, and the resolution of the z measurement (from the time difference) is 7.5 cm.

The luminosity of the colliding beams is determined by detecting small angle Bhabha scattering events with the forward detectors. These are lead-scintillator calorimeters with associated tracking chambers at either end of the central detector with an acceptance of $40 < \theta < 150$ mrad in polar angle and 2π in azimuth.

3 Global Event Selection and Quality Cuts

For the event selection, the tracking chambers, the forward detectors and electromagnetic calorimeters were required to be fully operational. Electromagnetic clusters consisted of groups of contiguous lead glass blocks, where each block registered an energy deposition of more than 20 MeV. A cluster was required to have a minimum energy of 170 MeV in the barrel and 250 MeV in the endcap region. Endcap clusters were required to contain a minimum of two adjacent blocks. In the barrel, a single block was sufficient to form a cluster.

Tracks were classified as 'good', and used in the analysis, provided they satisfied the following conditions:

- $|d_0| < 2.5$ cm, where $|d_0|$ is the distance of closest approach to the z-axis in the plane perpendicular to the axis.
- $|z_0| < 50$ cm, where $|z_0|$ is the distance to the nominal interaction point along the beam axis at the above point of closest approach.
- $N_{\rm hit} > 20$, corresponding to $|\cos\theta| < 0.97$, where $N_{\rm hit}$ is the number of hits in the jet chamber used to reconstruct the charged track. It was further required that the track contain more than 50% of the possible hits for a track at the given polar angle.
- $p_t > 100$ MeV/c, where p_t is the transverse momentum of the track with respect to the beam direction.

Events with low charge multiplicity were selected. They were required to contain at least one of the following:

- At least one track with $p_t \geq 1$ GeV/c, $|d_0| \leq 1$ cm and a total number of hits in the central tracking chambers greater than or equal to 30 out of a maximum possible of 183.
- Two electromagnetic clusters each with transverse energy greater than 6 GeV.

- Back-to-back electromagnetic clusters with an angle $\Delta\phi$ between their momentum directions in the plane perpendicular to the beam, in the range $155° \leq \Delta\phi \leq 205°$. One of the clusters must have an energy exceeding 2 GeV.

Further, it was required that there be less than 17 tracks and electromagnetic clusters in total.

4 Search for Four-Lepton Final States

Of the possible four-lepton final states, the four-τ final state has the lowest detection efficiency. The efficiencies for the detection of decays to electrons and muons are the same within errors.

In order to minimize potential background from hadronic events, and to exploit a simple low multiplicity topology for all final states, the following conditions were imposed:

- Only four-track final states were considered. As BR($\tau \rightarrow$ 1 charged track) = 85.8% [12], the maximum possible efficiency for a four-τ final state is 54.2%.
- The total charged track momentum $\Sigma|\vec{p}|$ was required to be greater than 20 GeV/c.

To reduce the background from two-photon interactions, it was demanded that:

- $E_{\rm FD} < 2$ GeV, where $E_{\rm FD}$ is the energy deposited in the forward detectors.

To reduce the background from beam-gas and beam-wall interactions, which contain a large number of tracks not coming from the interaction point, it was required that:

- $N_{\rm good}/N_{\rm all} > 0.20$, where $N_{\rm good}$ is the number of tracks in the event that satisfy the conditions of the previous section, and $N_{\rm all}$ is the total number of reconstructed charged tracks.
- $p_t > 1$ GeV/c and $|\cos\theta| < 0.9$ for all tracks in the event.
- The sum of the charges of the tracks in the event be equal to zero.
- The total electromagnetic energy, excluding energy inside cones of half-angle 15° centered on each track, be less than 3 GeV.

Of the 94 517 events defined by the low multiplicity event selection criteria of the previous section, 946 passed the cuts described above. The dominant background was expected to be from $Z^0 \rightarrow \tau^+\tau^-$. To check this expectation, the distribution of the minimum three-track invariant mass is shown in Fig. 1. The corresponding distribution expected for $\tau^+\tau^-$ events, simulated using the KORALZ Monte Carlo program [13] and subjected to the same cuts, is shown for comparison. Radiative Z^0 decays to leptons, with subsequent γ conversions, and four-lepton final states $\ell^+\ell^-l^+l^-$ – where ℓ and l can be electrons, muons or taus – were modelled according to references [13, 14, 15]. The contribution of these processes to the long tail of the three-track invariant mass distribution is also shown in Fig 1. The reasonable agreement between the distribution of the minimum three-track invariant mass obtained from the Monte Carlo simulation of the background, and that obtained from the data indicates that the background at this stage of the analysis was due predominantly to $\tau^+\tau^-$ events.

The following requirement was used to reduce the $\tau^+\tau^-$ background:

- The thrust axis, which was calculated using charged tracks, defined two hemispheres. Two tracks were demanded in each hemisphere.

Two events satisfied all requirements. One of these is consistent with being a hadronic decay of the Z^0, while the other is consistent with being a radiative dilepton event. This is to be compared with the expected background due to:

- Hadronic events: Approximately 171 000 Monte Carlo hadronic events (consisting of 105 850 events generated with JETSET [16], 20 492 events generated with Herwig [17] (version 43) and 18 747 events generated with Herwig (version 46)) run with the full detector simulation [18] were subjected to the analysis cuts listed above. Three events survived. Consequently, a background of 2.5 ± 1.4 events is expected from this source.
- $Z^0 \to \tau^+\tau^-$: The analysis cuts were applied to 20 000 Monte Carlo events of this type, generated using the KORALZ program with full detector simulation. Five events survived the cuts, giving rise to an estimated background of 1.5 ± 0.7 events from this source.
- Radiative leptonic decays of the Z^0 and four-fermion processes: Background from these sources was estimated using the following Monte Carlo programs: KORALZ for $Z^0 \to \mu^+\mu^-\gamma$, BABAMC [14] for $Z^0 \to e^+e^-\gamma$ and the Daverveldt program [15] for standard four-fermion processes. The background expected from these sources was 1.0 ± 1.0 event.

The above contributions combine to give an overall expected background of 5.0 ± 1.9 events, consistent with the two observed events.

The acceptance for the process $Z^0 \to H^{++}H^{--} \to \ell_1^+\ell_2^+\ell_3^-\ell_4^-(\ell = e, \mu, \tau)$ for the analysis cuts described was estimated using an event generator in which initial state radiation was taken into account [19]. The simulation of the detector response was modelled by smearing the generated track parameters to achieve agreement with the data.

A summary of the numbers of data events passing the analysis cuts, along with the effect of the same cuts on a sample of $H^{++}H^{--} \to \tau^+\tau^+\tau^-\tau^-$ ($M_H = 40$ GeV/c^2), is given in Table 2. Limits on $H^{\pm\pm}$ production are discussed in section 8.

5 Search for Long-Lived $H^{\pm\pm}$

For a small coupling of $H^{\pm\pm}$ to leptons ($g_{\ell\ell} \lesssim 10^{-7}$), the lifetime of the $H^{\pm\pm}$ is long enough for a substantial fraction of them to traverse the tracking chamber without decaying. A distinct signature of a long-lived $H^{\pm\pm}$ in the OPAL detector is a track with an ionization loss, dE/dx, significantly larger than that expected for a singly-charged track.

To look for long-lived $H^{\pm\pm}$ candidates that traverse the detector, the presence of an isolated track with an ionization loss consistent with that of a doubly-charged particle was required. In particular, the following demands were made on the events selected by the criteria of section 3:

- $p_t > 1$ GeV/c and $|\cos\theta| < 0.7$ for each track.
- The charged track multiplicity of the event was between one and nine inclusive.

- $\Sigma|\vec{p}| > 20$ GeV/c.
- $E_{\rm FD} < 2$ GeV.

A total of 12 867 events passed these selection criteria.

The dE/dx value was examined for the tracks of these events if they satisfied the following conditions:

- The track was separated from other tracks by at least 15°.
- $\sigma_{{\rm d}E/{\rm d}x}/({\rm d}E/{\rm d}x) < 10\%$, where $\sigma_{{\rm d}E/{\rm d}x}$ is the expected error on the mean dE/dx measurement of the track.

Figure 2 shows the dE/dx distribution for the 22 953 tracks passing these cuts. This distribution has a mean of 9.6 keV/cm and an average $\sigma_{{\rm d}E/{\rm d}x}$ of 0.43 keV/cm. The open histogram in Fig. 2 shows the dE/dx distribution for tracks in simulated decays $\rm Z^0 \to e^+e^-$, $\mu^+\mu^-$, $\tau^+\tau^-$ and hadrons. Both the width and the tails of the distribution for the data are well described by the Monte Carlo. Four data events are seen to have large values of dE/dx, corresponding to approximately twice the dE/dx of a minimum ionizing particle. The origin of such high dE/dx values is the unresolved overlap of two tracks of low dE/dx. The four events were scanned, and in each case the track with high dE/dx was found to be accompanied by activity in the tracking detector indicative of the presence of a nearby track. All four events are consistent with being of the type $\rm e^+e^- \to e^+e^-\gamma$, with the γ converting to an $\rm e^+e^-$ pair.

The shaded histogram shows the expected dE/dx distribution for a minimum ionizing $\rm H^{\pm\pm}$ ($M_{\rm H}$ = 11 GeV/c^2), which would deposit 31±3 keV/cm. This is well below the dE/dx value for which the detector saturates, which occurs at 20 times the dE/dx value for a minimum ionizing particle, or approximately 140 keV/cm.

The final requirement of the long-lived $\rm H^{\pm\pm}$ selection was the presence of a track with dE/dx greater than 22 keV/cm. No events satisfied this requirement.

6 Trigger Efficiency

In determining the efficiency for the detector to trigger on the process $\rm Z^0 \to H^{++}H^{--}$, the effects of the possible lifetimes, branching ratios to different charged leptons, and masses of the Higgs boson were considered, and the proportion of events satisfying the conditions for the OPAL detector to trigger was found. The cases of short-lived and long-lived $\rm H^{\pm\pm}$ were considered separately.

- Short-lived $\rm H^{\pm\pm}$: A Monte Carlo program was used to generate events with four-lepton final states ($\ell_1^+\ell_2^+\ell_3^-\ell_4^-$ where $\ell = e, \mu, \tau$) for $\rm H^{\pm\pm}$ with various masses and lifetimes. The conditions for the OPAL detector to trigger on these events with good efficiency were: 2 collinear TOF-ϕ sectors hit, ≥2 barrel tracks, 2 collinear tracks, or ≥1 track and a ϕ-correlated TOF sector hit. Overall efficiencies were found to vary between 96% and 100%. The value of 96% was used for the purpose of establishing limits.

- Long-lived $H^{\pm\pm}$: The efficiency to trigger on the two-track back-to-back topology of two $H^{\pm\pm}$ that exit the tracking chamber without decaying was greater than 94%. The efficiency for the single-track trigger (with correlated TOF counter hit) was 90%. The single-track trigger provided sensitivity to $H^{\pm\pm}$ with shorter decay lengths than the collinear track trigger if the particle was energetic enough to traverse the coil and strike a TOF counter. $H^{\pm\pm}$ with mass less than 42 GeV/c^2 would be sufficiently energetic to do so. A trigger efficiency of 90% was used in establishing the long-lived $H^{\pm\pm}$ limits.

7 Systematic Uncertainties

The following items contribute to the systematic uncertainty on the number of expected $H^{\pm\pm}$ events.

- Luminosity: a value of 0.8% was estimated for the error on the luminosity measurement [20].
- $H^{\pm\pm}$ cross section: the error on $\sin^2\theta_W = 0.2325 \pm 0.0008$ [12] corresponds to an error on the $H^{\pm\pm}$ cross section of $\pm 0.35\%$.
- Branching ratio: the error on BR($\tau \rightarrow$ one charged track) $= 0.8582 \pm 0.0025$ [12] corresponds to an error of $\pm 0.3\%$.
- Quality of the Monte Carlo simulation: the efficiencies to detect the $H^{\pm\pm}$ were measured using a Monte Carlo program which smeared the track parameters. The efficiencies obtained from this program agreed to within 3% with those obtained from a slower, well-tested Monte Carlo which performed full detector simulation and reconstruction [18]. A 3% systematic error was assigned due to the quality of the Monte Carlo simulation.
- Statistical error on the efficiency determination: the error on the $H^{\pm\pm}$ detection efficiencies were 2%, due to the limited size of the Monte Carlo event samples.
- The charged track multiplicity cut was the most important factor in determining limits. To test the sensitivity of the efficiency to the track quality, the required minimum number of hits on a track was varied by $\pm 10\%$. The error due to the $|d_0|$ and the $|z_0|$ cuts were examined. These sources were found to contribute negligibly to the error on the $H^{\pm\pm}$ detection efficiency.

A total systematic error of 4% was obtained by adding the above errors in quadrature.

8 Limits as a Function of Higgs Mass and $g_{\ell\ell}$

In the search for short-lived $H^{\pm\pm}$, the minimum number of expected events required to exclude the $H^{\pm\pm}$ at the 95% confidence level was calculated following the recommendation of the Particle Data Group [21]. With the expected number of background events taken as 3.1 (the number of expected background events reduced by one standard deviation) and with two observed events, this calculation yields a value of 4.4, which was used across the $H^{\pm\pm}$ mass range. Monte Carlo calculations were performed to determine the number of expected events as a function of $M_{\rm H}$ and $g_{\ell\ell}$. The number of expected events was reduced by 4% to take into account the systematic error on this number. The exclusion zone was taken to be the region in the $M_{\rm H}$-$g_{\ell\ell}$ plane for which the number of expected events was greater than 4.4.

The exclusion region for the process $Z^0 \to H^{++}H^{--} \to \ell_1^+\ell_2^+\ell_3^-\ell_4^-(\ell = e, \mu, \tau)$ for short-lived $H^{\pm\pm}$ is labeled as 'A' in Fig. 3. It extends from the $H^{\pm\pm} \to \ell_1^\pm\ell_2^\pm$ threshold to an upper limit of 45.6 GeV/c^2, primarily determined by the falling cross section for $Z^0 \to H^{++}H^{--}$. The boundary of the excluded region at small $g_{\ell\ell}$ in the four-lepton, short $H^{\pm\pm}$ lifetime search is determined by the efficiency of the four-track cut since, as $g_{\ell\ell}$ decreases, the $H^{\pm\pm}$ lifetime increases, and the fraction of events passing this cut falls. The exclusion zone is shown for both $I_3^L = \pm 1$ and $I_3^L = 0$.

The search for long-lived $H^{\pm\pm}$ includes the final states where one, or both, of the $H^{\pm\pm}$ escape the jet chamber without decaying. In this case, the mass range extends from twice the electron mass to an upper limit of 45.6 GeV/c^2. The upper $g_{\ell\ell}$ boundary of the excluded region is determined by the $H^{\pm\pm}$ lifetime: as $g_{\ell\ell}$ increases, the $H^{\pm\pm}$ lifetime decreases, and with it the likelihood that one of the $H^{\pm\pm}$ fully traverses the tracking chamber without decaying. The excluded region in the (M_H,$g_{\ell\ell}$) plane for this channel is labeled as 'B' in Fig. 3.

The exclusion regions for the short and long-lived $H^{\pm\pm}$ are insensitive to changes in the size of the data sample. For high mass, the edge of the regions is at the kinematic limit. As the acceptances for four tracks (in the short-lived $H^{\pm\pm}$ analysis), and for a $H^{\pm\pm}$ to traverse the entire detector (in the long-lived $H^{\pm\pm}$ analysis) fall rapidly to zero at values of $g_{\ell\ell}$ near the horizontal boundaries, these depend little on the number of $H^{\pm\pm}$ events expected. Doubling the data sample produces little change to the exclusion regions.

The existence of the decay mode $Z^0 \to H^{++}H^{--}$ would increase the total width of the Z^0 relative to the Standard Model prediction. Therefore, the value of $\Gamma_{Z^o}^{Meas}$- $\Gamma_{Z^o}^{SM}$ where $\Gamma_{Z^o}^{Meas}$ is the measured width of the Z^0 [22], and $\Gamma_{Z^o}^{SM}$ is the Standard Model prediction of the Z^0 width [23], gives a lower bound on the $H^{\pm\pm}$ mass. The prediction is a function of the unknown parameters α_s, M_t and M_{H^o} (the strong coupling constant, the top mass and the mass of the Standard Model Higgs boson). These were varied in the ranges $0.11 \leq \alpha_s \leq 0.13$, $89.0 \leq M_t \leq 200$ GeV/c^2 and $50.0 \leq M_{H^o} \leq 1000$ GeV/c^2, and the values that minimized $\Gamma_{Z^o}^{SM}$ were used to obtain a conservative limit. The difference between the measurement and the prediction is less than 40 MeV/c^2 at the 95% confidence level. The bound on the $H^{\pm\pm}$ width is obtained by setting the partial width for $Z^0 \to H^{++}H^{--}$ to 40 MeV/c^2 which yields a lower bound of 25.5 GeV/c^2 for $I_3^L = 0$, and 30.4 GeV/c^2 for $I_3^L = \pm 1$.

A small area for M_H greater than the lower bounds derived from Γ_{Z^o} is not excluded by either the short-lived or the long-lived search. This area corresponds to $H^{\pm\pm}$ lifetimes too short for the $H^{\pm\pm}$ to leave a sizeable track, but sufficiently long for the tracks of the decay products to fail the $|d_0|$ cut.

9 Conclusion

Using data taken during 1990 with the OPAL detector at LEP, a search has been made for a doubly-charged Higgs boson that decays dominantly via Yukawa couplings to two like-sign charged leptons, with short or long lifetime. Events with four charged leptons (corresponding to a large lepton coupling constant), and events where at least one of the doubly-charged Higgs bosons traverses the tracking chamber (corresponding to a small lepton coupling constant), have been sought. Two were found, consistent with the expected backgrounds. The two approaches, together with the measured width of the Z^0, were used to exclude the existence of the $H^{\pm\pm}$ with mass less than 45.6 GeV/c^2, and for values of $g_{\ell\ell}$ that extend down to zero.

10 Acknowledgements

It is a pleasure to thank the SL Division for the efficient operation of the LEP accelerator, the precise information on the absolute energy, and their continuing close cooperation with our experimental group. In addition to the support staff at our own institutions we are pleased to acknowledge the
Department of Energy, USA,
National Science Foundation, USA,
Science and Engineering Research Council, UK,
Natural Sciences and Engineering Research Council, Canada,
Israeli Ministry of Science,
Minerva Gesellschaft,
Japanese Ministry of Education, Science and Culture (the Monbusho) and a grant under the Monbusho International Science Research Program,
American Israeli Bi-national Science Foundation,
Direction des Sciences de la Matière du Commissariat à l'Energie Atomique, France,
Bundesministerium für Forschung und Technologie, FRG,
National Research Council of Canada, Canada,
A.P. Sloan Foundation and Junta Nacional de Investigação Científica e Tecnológica, Portugal.

References

[1] G. B. Gelmini and M. Roncadelli, Phys. Lett. **B99** (1981) 411.

[2] R. N. Mohapatra and J. D. Vergados, Phys. Rev. Lett. **47** (1981) 1713.

[3] V. Barger, H. Baer, W. Y . Keung and R. J. N. Phillips, Phys. Rev. **D26** (1982) 218.

[4] J. F. Gunion, H. E. Haber, G. L. Kane, and S. Dawson, The Higgs hunter's guide, (Addison-Wesley, 1990).

[5] ALEPH Collaboration, D. Decamp et al, Phys. Lett. **B241** (1990) 623;
DELPHI Collaboration, P. Abreu et al, Phys. Lett. **B241** (1990) 449;
L3 Collaboration, B. Adeva et al, Phys. Lett. **B252** (1990) 511;
OPAL Collaboration, M. Z. Akrawy et al, Phys. Lett. **B242** (1990) 299.

[6] J. A. Grifols, A. Mendez, and G. A. Schuler, Modern Physics Letters **A4** (1989) 1485.

[7] M. L. Swartz, Phys. Rev. **D40** (1989) 1521.

[8] D. Chang and W. Keung, Phys. Rev. Lett. **62** (1989) 2583;
F. Hoogeveen, Z. Phys. **C44** (1989) 259.

[9] Mark II Collaboration, M. Swartz et al., Phys. Rev. Lett. **64** (1990) 2877.

[10] F. A. Berends, G. Burgers and W.L. Van Neerven, Nucl. Phys. **B297** (1988) 429;
Erratum Nucl. Phys. **B304** (1988) 921;
O. Nicrosini and L. Trentadue, Phys. Lett. **B196** (1987) 551.

[11] OPAL Collaboration, K. Ahmet et al., Nucl. Instr. and Meth. **A305** (1991) 275.

[12] Review of Particle Properties, Particle Data Group, Phys. Rev. **D45** (1992).

[13] S. Jadach, B.F.L. Ward and Z. Was, Comp. Phys. Comm. **66** (1991) 276.

[14] M. Böhm, A. Denner and W. Hollik, Nuclear Physics **B304** (1988) 687;
F. A. Berends, R. Kleiss and W. Hollik, Nuclear Physics **B304** (1988) 712.

[15] F. A. Berends, P. H. Daverveldt and R. Kleiss, Phys. Lett. **B148** (1984) 489.

[16] T. Sjöstrand, Comp. Phys. Comm. **39** (1986) 347.

[17] G. Marchesini and B.R. Webber, Nucl. Phys. **B310** (1988) 461.

[18] OPAL Collaboration, J Allison et al, CERN-PPE 91-234 (1991).

[19] F. A. Berends and R. Kleiss, Nuclear Physics **B260** (1985) 32.

[20] OPAL Collaboration, G. Alexander et al., Z. Phys. **C52** (1991) 175.

[21] Expression 2.30, Review of Particle Properties, Particle Data Group, Phys. Rev. **D45** (1992) III.40.

[22] The LEP Collaborations, Phys. Lett. **B276** (1992) 247.

[23] D. Bardin et al., Comp. Phys. Comm. **59** (1990) 303;
D. Bardin et al., Z. Phys. **C44** (1989) 493;
D. Bardin et al., Nucl. Phys. **B351** (1991) 1;
D. Bardin et al., Phys. Lett. **B229** (1989) 405.

	$H^{\pm\pm}$ mass (GeV/c^2)										
	0.001	0.22	0.70	2.0	10	20	30	40	44	45	46
$I_3^L = \pm 1$	8444	8444	8442	8420	7840	6121	3592	920	149	39	2.6
$I_3^L = 0$	6128	6128	6126	6077	5690	4442	2607	668	108	28	1.9

Table 1: The number of $H^{\pm\pm}$ pairs expected as a function of the $H^{\pm\pm}$ mass and I_3^L for an integrated luminosity of 6.8 pb^{-1}.

Cut	Data events		$H^{\pm\pm}$ MC	
	Fail	Pass	Fail	Pass
Low mult. preselection	—	94517	2141	4859
Charge Multiplicity = 4	90849	3668	4179	2575
$\sum^{tracks} \vert\vec{p}\vert$ >20 GeV/c	66453	2239	1107	2123
Forward Energy < 2 GeV	21597	2187	197	2114
Good track fraction > 0.2	25311	2163	0	2114
Total charge = 0	37822	1837	1890	2085
p_t > 1 GeV/c (all tracks)	19394	1097	2971	1499
$\vert\cos\theta\vert$ < 0.9 (all tracks)	23996	1020	1678	1169
Unassociated E < 3 GeV	73419	946	1619	1010
Two tracks / hemisphere	34843	2	1273	969

Table 2: Comparison of the effects of the analysis cuts on the data and a sample of doubly-charged Higgs boson pairs decaying, with zero lifetime, to four taus. The columns entitled 'Fail' give the number of events failing each cut individually. Those entitled 'Pass' give the cumulative numbers of events passing each successive cut. The numbers of events in the column entitled '$H^{\pm\pm}$ MC' were calculated for $H^{\pm\pm}$ of mass 40 GeV/c^2, using the Monte Carlo program described in the text.

Figure 1: The minimum invariant three-track mass after all cuts except the topology cut demanding two tracks in each hemisphere. The points with error bars depict the invariant mass distribution for the data; the solid line shows the corresponding distribution for the sum of the backgrounds estimated from $\tau^+\tau^-$, $\ell^+\ell^-\gamma$ ($\ell = e, \mu$ or τ with the γ converting) and $\ell^+\ell^-l^+l^-$ (ℓ, l = e, μ, or τ) Monte Carlo events. The shaded region depicts the sum of the background processes $\ell^+\ell^-\gamma$ and $\ell^+\ell^-l^+l^-$ only.

Figure 2: The $\mathrm{d}E/\mathrm{d}x$ distribution for data, background and simulated $\mathrm{H}^{\pm\pm}$. The distribution of $\mathrm{d}E/\mathrm{d}x$ is shown for tracks selected as described in Section 5 (points with error bars). The open histogram shows the $\mathrm{d}E/\mathrm{d}x$ distribution for the simulated processes $\mathrm{Z}^0 \to \mathrm{e}^+\mathrm{e}^-$, $\mu^+\mu^-$, $\tau^+\tau^-$ and hadrons. The shaded section corresponds to the distribution of $\mathrm{d}E/\mathrm{d}x$ expected for minimum ionizing $\mathrm{H}^{\pm\pm}$ tracks.

Figure 3: The $\mathrm{H}^{\pm\pm}$ exclusion regions in the M_{H}-$\mathrm{g}_{\ell\ell}$ plane. The unhashed zones show the regions excluded at the 95% confidence level. The regions labeled by 'A' are excluded by the search for the short-lived $\mathrm{H}^{\pm\pm}$. Those labeled by 'B' (which extend down to $\mathrm{g}_{\ell\ell} = 0$) are excluded by the search for the long-lived $\mathrm{H}^{\pm\pm}$. $\mathrm{H}^{\pm\pm}$ with mass less than 25.5 GeV/c^2 ($I_3^L = 0$) or 30.4 GeV/c^2 ($I_3^L = \pm 1$) are excluded by measurements of Γ_{Z^0}, as indicated by the dotted lines.

Figure 1

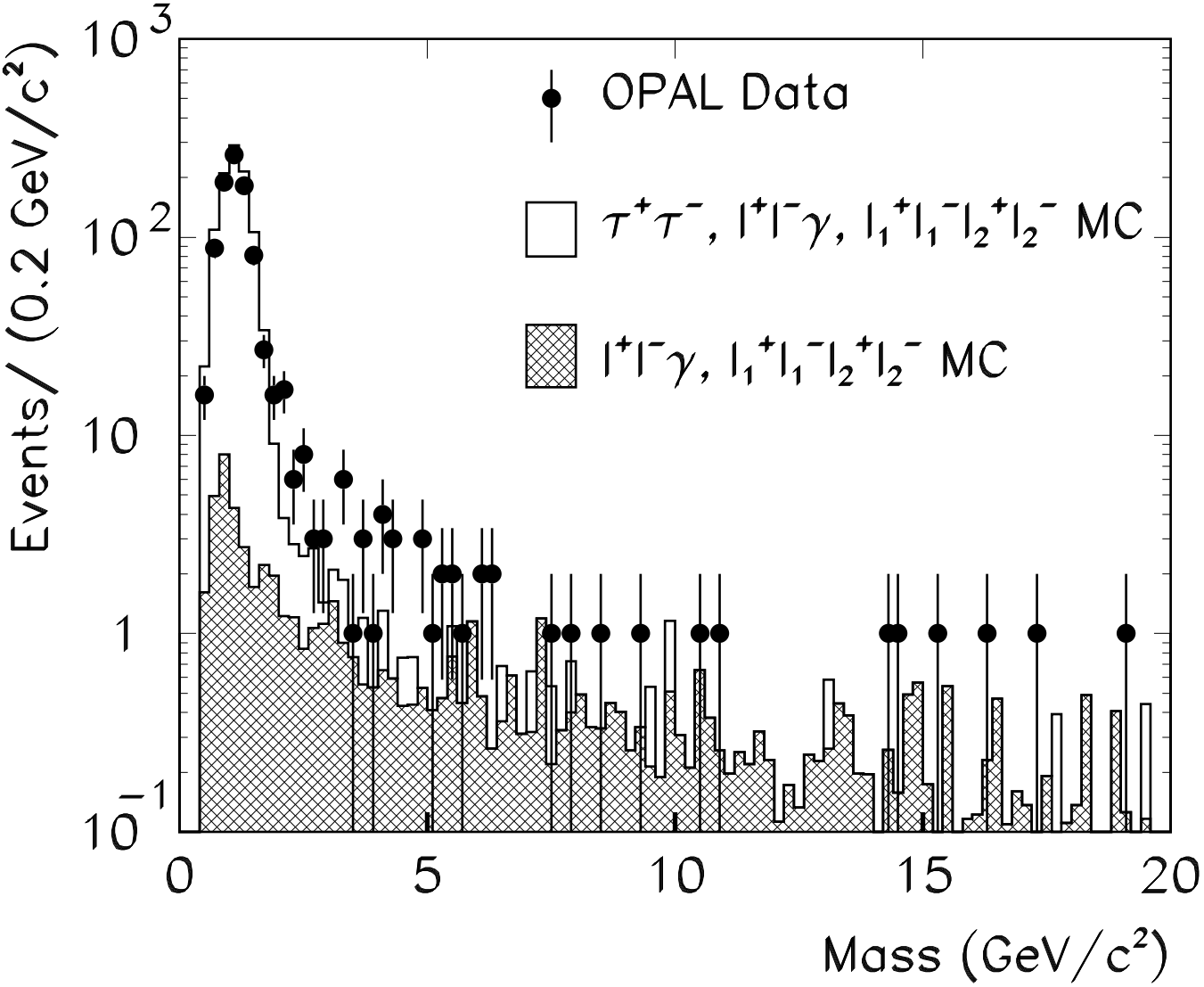
OPAL Data
$\tau^+\tau^-$, $l^+l^-\gamma$, $l_1^+l_1^-l_2^+l_2^-$ MC
$l^+l^-\gamma$, $l_1^+l_1^-l_2^+l_2^-$ MC
Events/ (0.2 GeV/c²)
Mass (GeV/c²)
10^3
10^2
10
1
10^{-1}
0
5
10
15
20

Figure 2

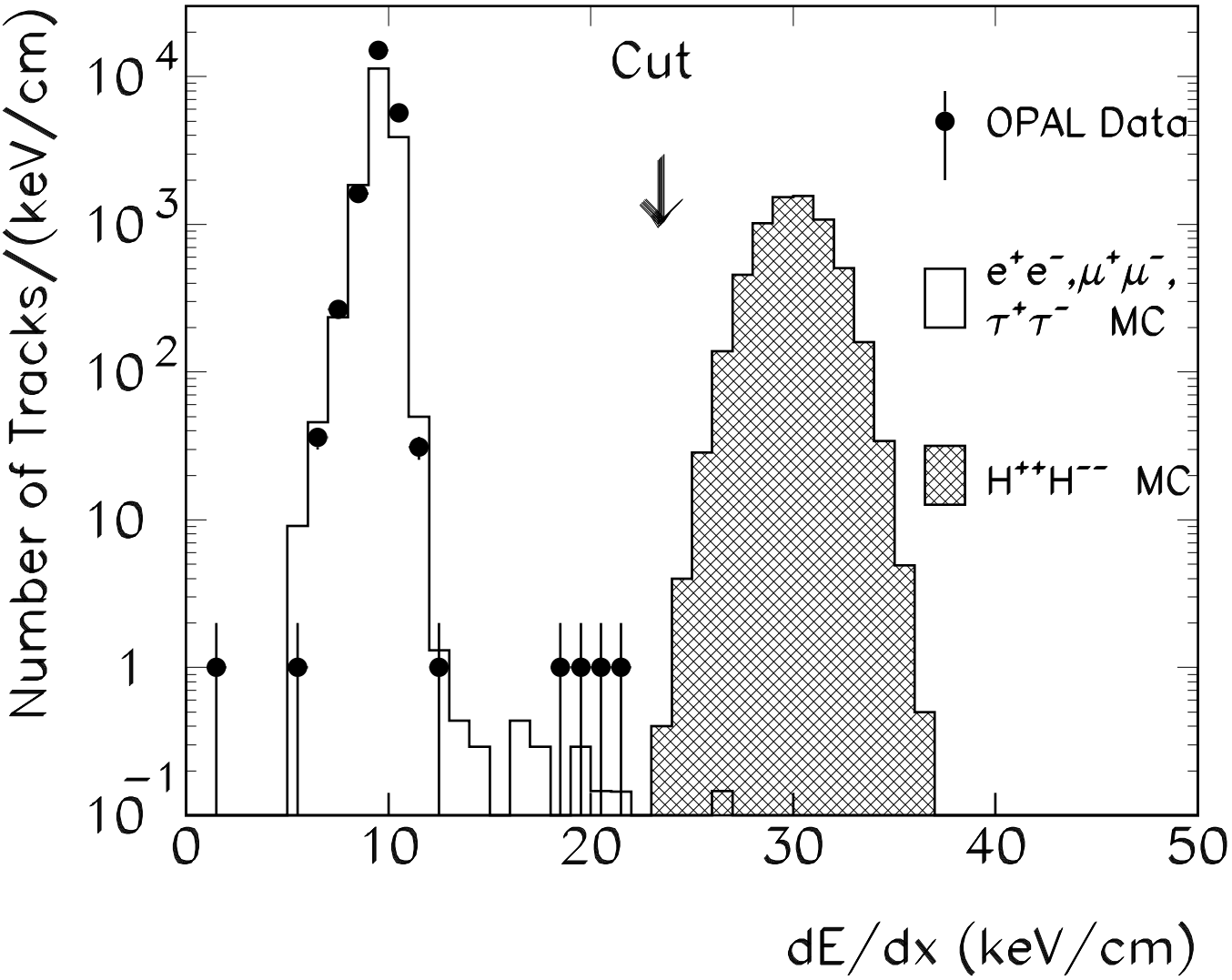
Number of Tracks/(keV/cm)
10^4
10^3
10^2
10
1
10^{-1}
0
10
20
30
40
50
dE/dx (keV/cm)
Cut
OPAL Data
$e^+e^-,\mu^+\mu^-,$
$\tau^+\tau^-$ MC
$H^{++}H^{--}$ MC

Figure 3

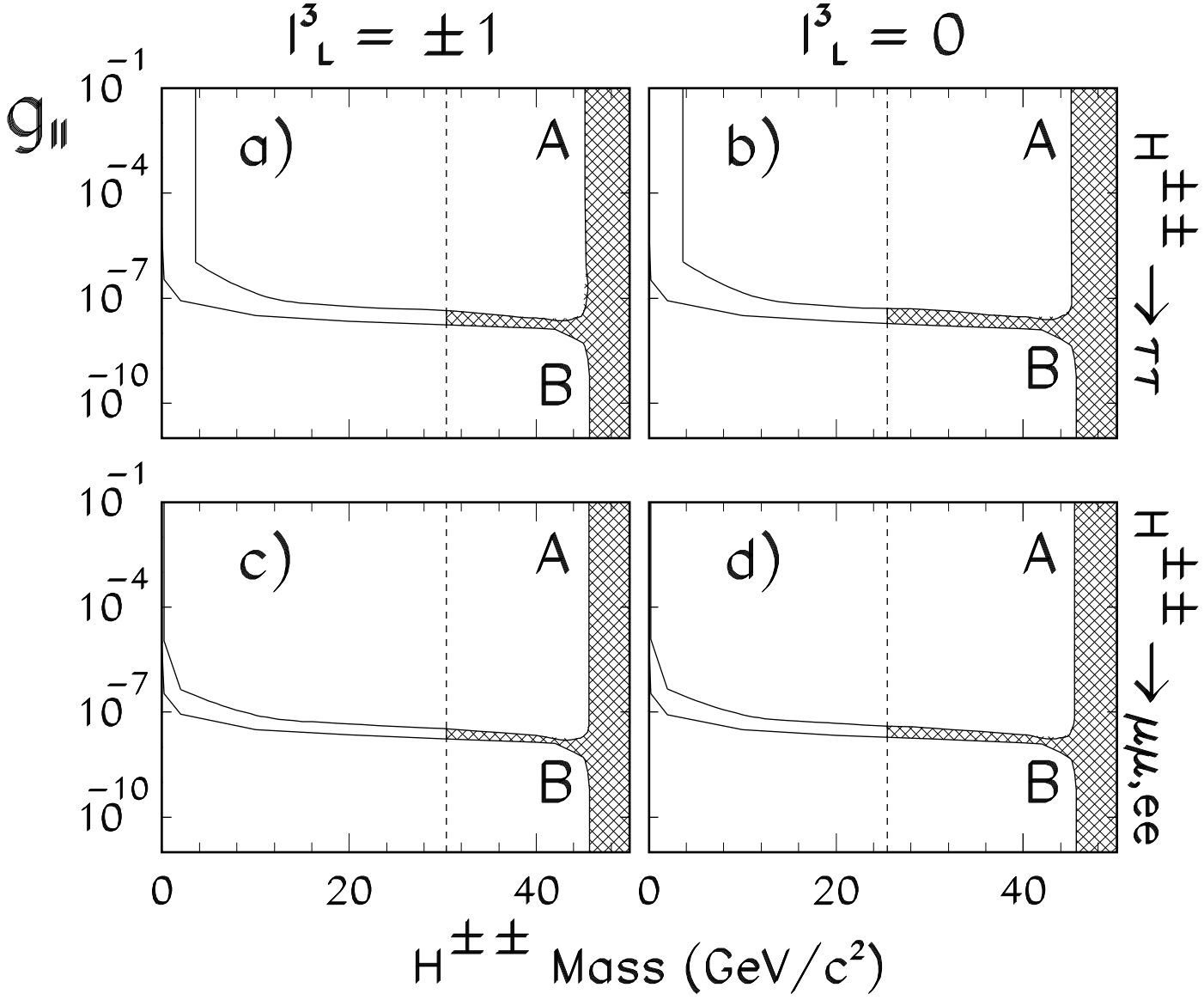
$I^3_L = \pm 1$
$I^3_L = 0$
g_{ll}
10^{-1}
10^{-4}
10^{-7}
10^{-10}
a)
b)
c)
d)
A
B
$H^{\pm\pm} \to \tau\tau$
$H^{\pm\pm} \to \mu\mu, ee$
0
20
40
$H^{\pm\pm}$ Mass (GeV/c^2)